



University of Pennsylvania
ScholarlyCommons

Departmental Papers (MEAM)

Department of Mechanical Engineering & Applied
Mechanics

1-1-2006

Evaluation of Some Thermal Power Cycles for Use in Space

Jason Tarlecki
University of Pennsylvania

Noam Lior
University of Pennsylvania, lior@seas.upenn.edu

Na Zhang
Chinese Academy of Sciences

Follow this and additional works at: http://repository.upenn.edu/meam_papers

 Part of the [Mechanical Engineering Commons](#)

Recommended Citation

Tarlecki, Jason; Lior, Noam; and Zhang, Na, "Evaluation of Some Thermal Power Cycles for Use in Space" (2006). *Departmental Papers (MEAM)*. 262.
http://repository.upenn.edu/meam_papers/262

Suggested Citation:

Tarlecki, J., Lior, N. and Zhang, N. (2006). "Evaluation of Some Thermal Power Cycles for Use in Space." *Proc. ECOS 2006*. Crete, Greece. 12-14 July 2006.

This paper is posted at ScholarlyCommons. http://repository.upenn.edu/meam_papers/262
For more information, please contact libraryrepository@pobox.upenn.edu.

Evaluation of Some Thermal Power Cycles for Use in Space

Abstract

Production of power in space for terrestrial use is of great interest in view of the rapidly rising power demand and its environmental impacts. Space also offers a very low temperature, making it a perfect heat sink for power plants, thus offering much higher efficiencies. This paper focuses on the evaluation and analysis of thermal Brayton, Ericsson and Rankine power cycles operating at space conditions on several appropriate working fluids. 1. Under the examined conditions, the thermal efficiency of Brayton cycles reaches 63%, Ericsson 74%, and Rankine 85%. These efficiencies are significantly higher than those for the computed or real terrestrial cycles: by up to 45% for the Brayton, and 17% for the Ericsson; remarkably 44% for the Rankine cycle even when compared with the best terrestrial combined cycles. From the considered working fluids, the diatomic gases (N₂ and H₂) produce somewhat better efficiencies than the monatomic ones in the Brayton and Rankine cycles, and somewhat lower efficiencies in the Ericsson cycle. The Rankine cycles require radiator areas that are larger by up to two orders of magnitude than those required for the Brayton and Ericsson cycles. The results of the analysis of the sensitivity of the cycle performance parameters to major parameters such as turbine inlet temperature and pressure ratio are presented, and the effects of the working fluid properties on cycle efficiency and on the power production per unit radiator area were explored to allow decisions on the optimal choice of working fluids.

Keywords

Power cycles, Space power, Space, Brayton cycle, Ericsson cycle, Rankine cycle

Disciplines

Engineering | Mechanical Engineering

Comments

Suggested Citation:

Tarlecki, J., Lior, N. and Zhang, N. (2006). "Evaluation of Some Thermal Power Cycles for Use in Space." *Proc. ECOS 2006*. Crete, Greece. 12-14 July 2006.

EVALUATION OF SOME THERMAL POWER CYCLES FOR USE IN SPACE

Jason Tarlecki and Noam Lior*

Department of Mechanical Engineering and Applied Mechanics
University of Pennsylvania
Philadelphia, Pennsylvania 19104-6315, USA

Na Zhang

Institute of Engineering Thermophysics
Chinese Academy of Sciences
Beijing 100080, China

ABSTRACT Production of power in space for terrestrial use is of great interest in view of the rapidly rising power demand and its environmental impacts. Space also offers a very low temperature, making it a perfect heat sink for power plants, thus offering much higher efficiencies. This paper focuses on the evaluation and analysis of thermal Brayton, Ericsson and Rankine power cycles operating at space conditions on several appropriate working fluids. 1. Under the examined conditions, the thermal efficiency of Brayton cycles reaches 63%, Ericsson 74%, and Rankine 85%. These efficiencies are significantly higher than those for the computed or real terrestrial cycles: by up to 45% for the Brayton, and 17% for the Ericsson; remarkably 44% for the Rankine cycle even when compared with the best terrestrial combined cycles. From the considered working fluids, the diatomic gases (N_2 and H_2) produce somewhat better efficiencies than the monatomic ones in the Brayton and Rankine cycles, and somewhat lower efficiencies in the Ericsson cycle. The Rankine cycles require radiator areas that are larger by up to two orders of magnitude than those required for the Brayton and Ericsson cycles. The results of the analysis of the sensitivity of the cycle performance parameters to major parameters such as turbine inlet temperature and pressure ratio are presented, and the effects of the working fluid properties on cycle efficiency and on the power production per unit radiator area were explored to allow decisions on the optimal choice of working fluids.

Keywords: Power cycles, Space power, Space, Brayton cycle, Ericsson cycle, Rankine cycle

Nomenclature

A	Area [m^2]	s	Specific entropy [kJ/kg·K]
a	Exergy [kJ/kg]	t	Radiator wall thickness [m]
c	Speed of sound [m/s]	T	Temperature [K]
G	Mass flow rate [kg/s]	TIT	Turbine inlet temperature [K]
h_c	Convective heat transfer coefficient [$W/m^2 \cdot K$]	U	Overall heat transfer coefficient [$W/m^2 \cdot K$]
h_r	Radiative heat transfer coefficient [$W/m^2 \cdot K$]	W	Power output [kW]
k	Thermal conductivity constant [$W/m \cdot K$]	w	Specific power output [kJ/kg]
Nu	Nusselt number	Greek	
p	Pressure [bar]	δ	Radiator flow gap [m]
Pr	Prandtl number	ΔT_{lm}	Log mean temperature difference [K]
Q	Heat duty [kW]	ϵ	Emissance
Re	Reynolds number	ϵ	Exergy efficiency
R_t	Total thermal resistance [K/W]	η_t	Thermal efficiency
		π	Pressure ratio
		σ_{sb}	Stefan-Boltzmann constant [$5.67(10^8)$]

* Corresponding author: Phone: +1 215 898 4803 Fax: +1 215 573 6334 Email: lior@seas.upenn.edu

	W/kg·K ⁴
Ψ	Power produced per unit radiator area [kW/m ²]

Subscripts

<i>in</i>	Inlet
<i>out</i>	Outlet
<i>H</i>	High
<i>L</i>	Low
<i>rad</i>	Radiator
<i>s</i>	Space
<i>t</i>	Total
1..10	States on the cycle flow sheet

INTRODUCTION

Power from space

In view of the worrisome fact that the world population is expected to double and the demand for electricity to increase 16-fold in the next 50 years [1-3], it was recognized over the past few decades by various scientific and aerospace experts and institutions [1-3] that space offers numerous advantages as a site for power production. In addition to the better known proposal to generate power in space by using photovoltaic converters [1], space is also an ideal, near-zero K, heat sink for thermal power generation, and can thus offer Carnot efficiencies close to 100% [3]. Exploiting this low temperature in space, working fluids can be used in the power plant (such as inert gas mixtures), even to condensation in the Rankine cycle.

Some of the most probable heat sources are solar and nuclear. Using the sun as the primary energy source of the power plant only further boosts the advantages of power from space solar power, which requires a collection area about 8-fold smaller than that needed on earth [1,4-6]. Nuclear energy, already used for satellite and space probe powering in space over the last 30 years, is also an option for space.

Some of the most likely methods for transmitting the generated energy to earth are microwave or laser beaming, and transportation of energy-rich materials. It will also be more efficient to beam this power to developing countries and regions, instead of building new power lines, similar to how cellular phones have surpassed conventional telephones in these regions (cf. [7,8]).

Precious terrestrial surface that would have been used for situation of power plants, especially large where renewable energy is planned to be

used, is saved. There are also no terrestrial pollution consequences.

The objective of this study: analysis of thermal power cycles for use in space

This paper deals with one aspect of space power generation: the analysis of performance of recuperative Brayton, Ericsson, and Rankine thermal power cycles that operate under space conditions. The heat source could be any, most likely solar or nuclear, and space is the heat sink.

The primary obstacle to commercial use of space power is the high cost of the produced power, which, in turn, is strongly affected by the system weight because sending the systems into space with currently available launch systems is a dominant fraction of the total cost [9,10]. For a desired net power output, increasing the thermal system energy conversion efficiency reduces both the cost of the heat input system (solar concentrator and receiver, or nuclear reactor) and the amount of heat that must be rejected (and thus the size and weight of the radiator). At the same time, reduction of the working fluid temperature in the radiator increase the thermal efficiency but decreases the heat rejection temperature difference and consequently increases the needed radiator size/weight, requiring optimization of that temperature.

The system orbit or space platform (such as the moon) affect insolation, space temperature, and eclipse time (during which solar powered systems do not receive radiation), as well as transmission to earth, but in this paper we focus on the energy and exergy efficiency and the associated specific area of the radiator and do not consider orbit effects.

The temperature and pressure of space are needed for setting the heat sink temperature, designing of the heat-rejection radiator, and establishing the dead state in the exergy analysis. Currently, astronomers agree that the cold temperature of space is about 3 K. In this analysis, it is estimated to be 2.7 K due to background microwave radiation [11,12], but varying the temperature by a few degrees does not affect the results significantly. This temperature is assumed here to be the lowest that space can offer and is thus useful for estimating the maximal thermodynamic potential of space, and is used here as the dead state temperature for the exergy analysis. It is noteworthy though that the effective temperature depends on the radiative exposure to nearby objects, and the literature shows use of space temperatures from 0K [13] to 223K [10], with a value of ~190K used often.

The pressure environment is complex and can fluctuate substantially. At a height of 320 km (in Low Earth Orbit, LEO) from Earth's surface, an orbiting object can be in a pressure field varying between 10^{-8} bar in the front to 10^{-10} bar in the rear due to collisions with the ambient atmosphere. Assuming an orbital velocity of about 8 km/s, the dead state pressure (p_o) becomes 10^{-8} bar [14].

The top cycle temperatures were selected to be those employed in conventional power plants, and somewhat beyond, to address expected increases as technology keeps developing. The very low bottom cycle temperature (below 100 K in Rankine cycles) and the correspondingly high temperature ratio make the performance of these cycles rather interesting.

Three primary performance criteria were used for evaluating and comparing the different cycles and working fluids: the energy efficiency η , the exergy efficiency ε (very useful for helping find ways to improve cycle performance), and the ratio of the power output to required radiator area, Ψ [kW/m^2], which are defined, respectively, as

$$\eta_I = \frac{w_{net}}{Q_{in}} \quad (1)$$

$$\varepsilon = \frac{w_{net}}{(a_{out} - a_{in})_{heat-addition}} \quad (2)$$

$$\Psi = \frac{Gw_{net}}{A_{rad}} \quad (3)$$

RADIATOR ANALYSIS

The conceived radiator for all three cycles is of a flat-plate design. It is assumed that the radiators will be constructed of aluminum, to cohere with similar space power structures [15,16]. The necessary radiator area needed to reject the heat rate Q_{out} is calculated from

$$A_{rad} = \frac{Q_{out}}{U\Delta T_{lm}} \quad (4)$$

The overall heat transfer coefficient (U) is calculated from

$$U = \frac{1}{R_t A} = \frac{1}{t/k + 1/h_c + 1/h_r} \quad (5)$$

where k is the thermal conductivity of the plate, t its thickness, h_c the convective heat transfer coefficient, and h_r the radiative heat transfer coefficient calculated here by

$$h_r \equiv \epsilon \sigma_{sb} (\Delta T_{lm} + T_s)(\Delta T_{lm}^2 + T_s^2) \quad (6)$$

The required size of the radiators is calculated from Eq. (4), rewritten as

$$A_{rad} = \frac{Gc_{p,6-1}(T_6 - T_1)}{U\Delta T_{lm}} \quad (7)$$

Using Eqs. (3), (7), and (1), Ψ can be expressed as

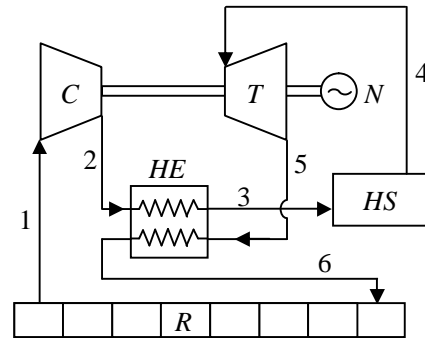
$$\Psi = \frac{Gw_{net}}{A_{rad}} = U\Delta T_{lm} \frac{w_{net}}{q_{out}} = U\Delta T_{lm} \frac{1}{\frac{1}{\eta_I} - 1} \quad (8)$$

indicating, as expected, that Ψ will decrease if U and ΔT_{lm} , are increased, and if the energy efficiency of the cycle, η_I , is increased. Equation (8) is strictly valid for Brayton and Rankine cycles only, as the Ericsson cycle has multiple radiators, with varying ΔT_{lm} and U throughout multiple stages of heat rejection.

CYCLE CONFIGURATIONS

The configurations for the Brayton, Ericsson and Rankine cycles analyzed in this paper are shown in Figs. 1, 2, and 3, respectively. Since this is just an initial study, simple configurations were chosen. The Brayton cycle is self-explanatory. In the *Ericsson* cycle, a high temperature and pressure gas at state (1) enters a multistage turbine (*MT*) and is expanded and reheated multiple times until the entire process approaches constant temperature expansion and reaches state (2). Here the gas enters the regenerator (*HE*) where the heat remaining from the constant temperature expansion is transferred to the cooler gas at state (5). At state (3), the gas is further cooled in the radiator (*R*) to state (4). Then the gas enters a multistage compressor (*MC*) where it is compressed and intercooled several times to mimic constant temperature compression. At state (5), the gas enters the *HE*, is heated to state (6), then is further heated in a heat source generator (*HS*) until reaching its original state (1).

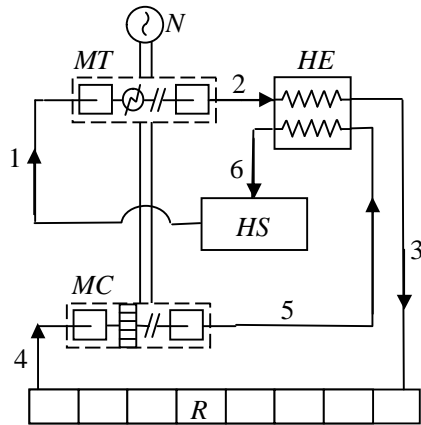
The *Rankine* cycle is perhaps the most interesting of the three explored, because the low temperature of space is used to liquefy the inert



C— Compressor T— Turbine HE— Heat Exchanger
N— Generator HS— Heat Source R— Radiator

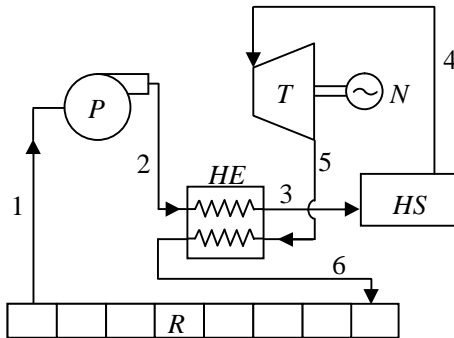
Fig. 1: Brayton cycle flow sheet

gases used, resulting in the lowest required back



MC— Multistage Compressor w/ Intercooling
 MT— Multistage Turbine w/ Reheating N— Generator
 HE— Heat Exchanger HS— Heat Source R— Radiator

Fig. 2: Ericsson cycle flow sheet



P— Pump T— Turbine HE— heat exchanger
 N— Generator HS— Heat Source R— Radiator

Fig. 3: Rankine cycle flow sheet

work ratio.

SELECTION OF WORKING FLUIDS

Based on past work on space thermal power cycles [15-20], the working fluids investigated for the Brayton and Ericsson cycles are argon (Ar), nitrogen (N₂), argon-xenon (Ar-Xe, 50% Ar by

weight), helium (he), helium-xenon (He-Xe, 50% He by weight), and hydrogen (H₂). Only the first two fluids were considered for the Rankine cycle.

Brayton and Ericsson cycle performance improves significantly as the compressor inlet temperature decreases, and to take the advantage of the very low heat sink temperature that space offers, the working fluids in gas cycles should have low condensation temperatures at the cycle low pressure.

In the Rankine cycle, the working fluid should have a low triple point temperature and pressure, to take the advantage of the low heat sink temperature and enlarge the possible working area of the fluid. Some of the properties are in Table 1.

PERFORMANCE OF CYCLES

Cycle definitions and analysis method

To compute these and all the other system parameters, simulations of the systems were carried out using the Aspen Plus commercial software package [21], with a computing error of 10⁻⁵. Irreversibilities included in this analysis are both internal and external. All heat transfer through finite temperature differences and expansions of liquids and gases to lower pressures have been accounted for. The pressure drops in the pipes were ignored to keep this analysis relatively simple and as close to ideal as possible. From power plant practice, they would be within roughly 3% pressure drop only anyway. All the conditions and results are shown in Table 2.

Regeneration temperatures are determined by the compressor and turbine exit temperatures for Brayton and Ericsson cycles, and by the turbine exit temperature and pinch point for the Rankine cycle. HE effectiveness is chosen as 0.9 and is utilized in Brayton and Ericsson cycles. However, in the Rankine cycle, an effectiveness of 0.9 cannot be achieved due to existence of liquid on the hot side of the HE (T₂ to T₃), causing the two stream temperatures to arrive at a pinch point before reaching the desired effectiveness. Thus, in the Rankine cycle, a minimal temperature difference of 15 K is chosen.

Table 1: Major properties of the working fluids for the conditions of the analyzed Brayton and Ericsson cycles.

The working fluid:	Ar	He	Xe	Ar-Xe	He-Xe	N ₂	H ₂
Condensation	T, K	84.5	-	-	-	64.2	-
	P, bar	0.75	-	-	-	0.15	-
Triple point	T, K	83.80	2.17	161.3	-	63.15	13.95
	P, bar	0.69	0.05	0.82	-	0.13	0.07
Critical point	T, K	150.7	5.20	289.7	-	126.2	33.19
	P, bar	48.6	2.27	58.4	-	34.0	13.2
Atomic mass	39.95	4.00	131.29	61.26	7.76	28.01	2.02

Table 2: All cycle parameters and results

			Brayton	Ericsson	Rankine	
					Ar	N ₂
Cycle Parameter		p_L [bar]	1	1	0.75	0.15
		T_L [K]	200	200*	84	64
Compression Stage		π	8	8	200	1000
Results	η_I	Ar	0.5826	0.7360	0.7788	
		Ar-Xe	0.5829	0.7372	-	
		N ₂	0.6339	0.6880	0.8461	
		He	0.5818	0.7339	-	
		He-Xe	0.5819	0.7339	-	
		H ₂	0.6322	0.6945	-	
	ε	Ar	0.5841	0.7374	0.7828	
		Ar-Xe	0.5844	0.7385	-	
		N ₂	0.6354	0.6892	0.8496	
		He	0.5833	0.7352	-	
		He-Xe	0.5833	0.7353	-	
		H ₂	0.6337	0.6957	-	
	Ψ [kW/m ²]	Ar	0.9958	0.3104	0.01435	
		Ar-Xe	0.9947	0.3083	-	
		N ₂	0.8683	0.2913	0.00816	
		He	1.0014	0.3150	-	
		He-Xe	1.0013	0.3149	-	
		H ₂	0.8499	0.2959	-	

$G = 350$ kg/hr, $\eta_s = 90\%$ (turbine), $\eta_s = 85\%$ (compressor, pump), $TIT = 1500$ K

* Average temperature during compression with intercooling

Power generation

Figure 4 shows the dependence of the energy efficiency and of Ψ , and Fig. 6 of the exergy efficiency, on the pressure ratio (π), respectively, for a range of turbine inlet temperatures TIT (the highest values exceed conventional practice but are included to examine the potential that would result from further improvements in turbine technology). On these graphs, the solid markers represent Brayton cycle with regeneration, and hollow markers show the results at which the specific pressure ratios do not allow regeneration. With regeneration, the cycle yields energy and exergy efficiencies of over 65% in the lower pressure ratio range; without regeneration they still reach over 55%. There clearly is a value of π giving a maximal energy efficiency for a given TIT . This fact is well known for Brayton cycles, and occurs because isobars, for all fluids, diverge as both T and s increase. Simple examination of the T - s representation of Brayton cycles without regeneration shows that when operating between top and bottom fixed temperatures (T_L and T_H), Q_{in}

decreases as π increases since compressor exit temperature approaches T_H . In Brayton cycles with regeneration, the turbine exhaust temperature is higher for lower pressure ratios, and thus brings the combustion inlet stream to a higher temperature or reduces the heat input required. The ratio in Eq. (1) first increases with π , due to the larger divergence of the isobars at low π (between fixed temperatures T_L and T_H); but as π becomes so large that the compressor exit temperature approaches TIT , w_{in} approaches w_{out} , causing w_{net} to rapidly approach zero and energy efficiency to decrease to zero. The saddle points on each curve show the transition between a Brayton cycle when regeneration is in effect (left hand side) and a Brayton cycle when regeneration ceases to be possible (right hand side). Brayton cycles without regeneration behave the same as cycles utilizing regeneration (with an optimal π giving maximum energy efficiency for each TIT), but the maximal efficiencies occur at higher π than in regenerative cycles. Thus, at certain higher π ,

using no regeneration yields higher efficiencies, causing the saddle point in Fig. 4.

In the Brayton cycles with lower pressure ratio, $T_2 < T_5$ and heat is transferred in the regenerator from process 5-6 to 2-3. This helps increase the *HS* cold stream inlet temperature (state 3 in Fig. 1), and therefore reduce the heat demand in *HS* and increase the efficiencies. When π is increased, the temperature T_2 will increase while T_5 will decrease until T_2 and T_5 thus become equal to each other, preventing any heat transfer (heat recovery) in *HE*. At this π the Brayton cycle with and without regeneration have the same efficiencies. When π is increased further, T_2 becomes larger than T_5 causing the regenerator *HE* to actually cause bigger heat demand in *HS* and reduce the efficiencies (obviously, *HE* would not be used for these conditions).

The same cycle parameters are used in the Ericsson and Brayton cycles for easy comparison. The number of expansion and compression stages in turbines and compressors, respectively, was chosen by gradually increasing them and examining the effect on the energy efficiency. It was found that the energy efficiency increase tapers off as the number of stages increases; after the sixth stage, it only increases approximately 0.1% per stage added. All Ericsson cycles in this analysis thus have six interstages in both the compressor and turbine.

Sample results are shown in Fig. 5 for a nitrogen Rankine cycle defined in Table 2. The thermal efficiency of the Rankine cycle increases, as expected, with increasing *TIT*, and insignificantly with increasing π . The Rankine cycle has much higher energy and exergy efficiencies than the Brayton and Ericsson ones, reaching over 85% at the highest π , because of the much lower back-work ratio (see Table 3).

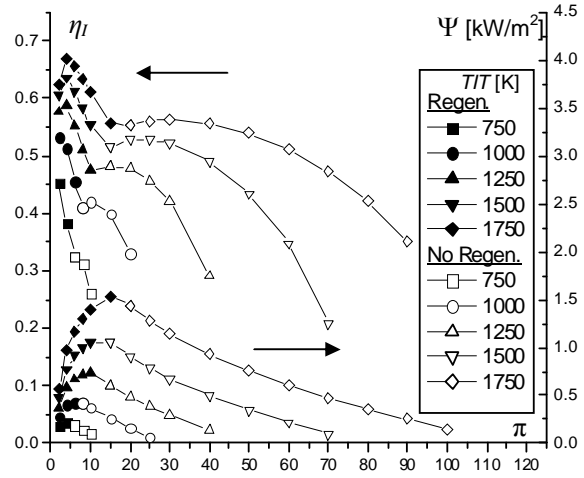


Fig. 4 Effect of pressure ratio on thermal efficiency and Ψ , argon Brayton cycle, $p_L=1$ bar

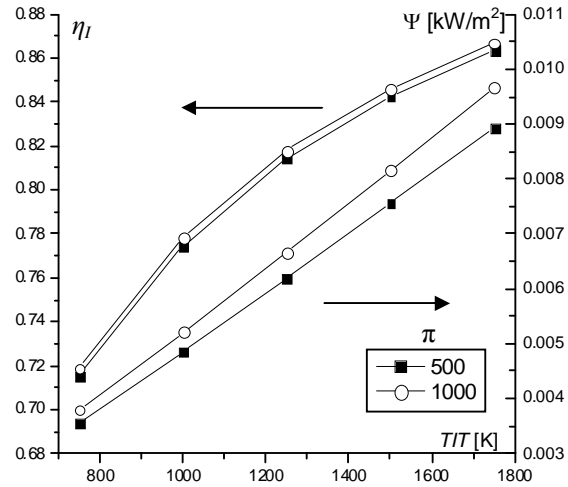


Fig. 5: Effect of *TIT* on thermal efficiency, nitrogen Rankine cycle, $p_L=0.15$ bar

Table 3: Back-work ratio, all cycles and working fluids [%]

Cycle	Ar	Ar-Xe	N ₂	He	He-Xe	H ₂
Brayton	39.94%	39.86%	30.31%	40.05%	40.05%	31.27%
Ericsson	17.12%	16.99%	17.17%	17.34%	17.33%	17.37%
Rankine	2.00%	N/A	1.57%	N/A	N/A	N/A

Radiator requirements

The analysis is conducted using Eqs. (3)-(8). It is assumed that $\epsilon = 1$, and fluid velocity of 1/3 the speed of sound. The main conditions and results are shown in Table 4. It is noteworthy that the radiative heat transfer resistance is larger than the

others by at least an order of magnitude. Since that resistance depends primarily on the radiator temperature, the resistances in the Rankine cycle, which are up to 2 orders of magnitude higher than those in the other cycles, reflect the lower radiator temperature in that cycle.

Table 4: Properties used in development of h_c , Brayton and Ericsson cycles

Property	Ar	Ar-Xe	N ₂	He	He-Xe	H ₂
c [m/s]	351	283	351	1106	794	1315
$c/3$ [m/s]	117	94	117	369	265	438
$Re \times 10^{-4}$	4.11	4.94	3.69	1.48	1.85	1.98
Pr	0.66	0.57	0.71	0.69	0.42	0.71
Nu	95.7	104.7	90.5	43.1	42.4	54.9
h_c [W/m ² -K]	344	293	471	1292	1188	1976

COMPARISON OF WORKING FLUID EFFECTS ON SYSTEM PERFORMANCE

Since a sensitivity analysis of the Brayton cycle showed that the highest energy efficiencies and Ψ are obtained at about $TIT=1500$ K (the highest for all working fluids) and $\pi=8$, the comparison between the Brayton and Ericsson cycles is conducted up to these temperature and pressures. Sample T - s diagrams for the different working fluids of the Brayton cycle are shown in Figs. 6 and 7. An Ericsson cycle T - s diagram is shown in

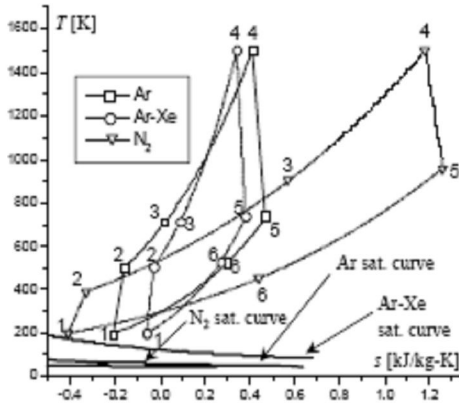


Fig. 6: Brayton cycle T - s diagram (Ar, Ar-Xe, and N₂), $P_1=1$ bar, $\pi=8$

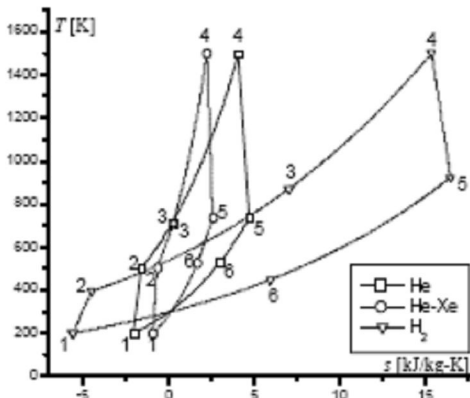


Fig. 7: Brayton cycle T - s diagram (He, He-Xe, and H₂), $P_1=1$ bar, $\pi=8$

Fig. 8, and it is important to note that this cycle configuration is specific to this analysis and that Ericsson configurations can vary based on number of interstages in the turbine and compressor. The Rankine cycle has the highest η_I and Ψ at $TIT=1500$ K and $p_H=150$ bar which are the base parameters for comparisons (note: this implies $\pi=200$ for Ar and $\pi=1000$ for N₂). Further increase in π does not significantly increase η_I (see Fig. 5): doubling π only increases η_I by 0.3%. η_I , ϵ , and Ψ all increase with increasing TIT and π for both working fluids used in the Rankine cycle. Sample T - s diagrams for the Rankine cycle are shown in Fig. 9. Fig. 10 shows a summary of the performance results.

Compared with computed cycles operating under terrestrial conditions, the space cycles are more efficient, as expected due to the lower temperature heat sink. In addition, the Brayton cycle using Ar, Ar-Xe, He, and He-Xe, operating at the lower temperature of space allows regeneration otherwise impossible at terrestrial conditions due to temperature constraints. As a result, efficiencies increase by 45%. Likewise, N₂ and H₂, using regeneration both in space and on earth, have efficiency increases of over 28%. Similarly, Ericsson cycles gain an efficiency increase of over 14% for all working fluids considered when operating in space. Although yielding higher efficiencies both in space and on Earth, Ericsson cycles have a slightly lower increase in efficiency because they are already highly efficient in being close to the ideal Carnot cycle by design (52-56% thermal efficiency at terrestrial conditions). Currently, state of the art operating terrestrial power plants have thermal efficiencies of 40% for gas turbine power (100 MW) amazingly close to those predicted in our simplified analysis (Table 2), nearly 50% for conventional steam power plant (1000 MW), and 60% for a combined cycle (1000 MW) [19,20], all lower than the predicted space power cycles. It is noteworthy that a space Rankine cycle is predicted to attain efficiency in the range of 80% just by

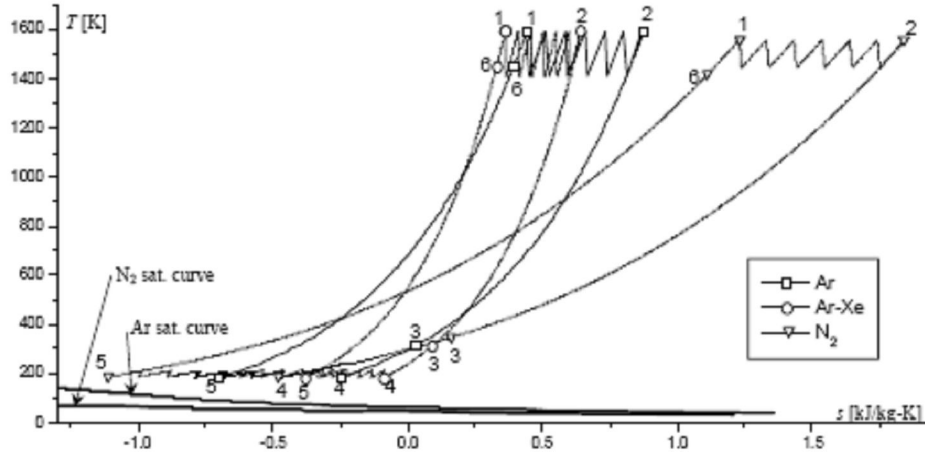


Fig. 8: Ericsson cycle T - s diagram (Ar, Ar-Xe, and N_2), $P_L=1$ bar, $\pi=8$

itself, not in a combined configuration. A combined configuration is unnecessary anyway because the heat rejection is at the lowest possible temperatures.

Aside from the Brayton terrestrial cycles with compressor exit temperatures that are too high to use regeneration (monatomic gases), all terrestrial cycles have higher exergy efficiencies compared to their respective space cycle (Table 2). Comparison of the exergy efficiency of terrestrial and space cycles is not straightforward, because of the different dead states used for them: $T_o=288.2$ K for terrestrial cycles, and $T_o=2.7$ K for space. Some interesting conclusions can be drawn though: examination of the exergy efficiency definition, Eq. (2), leads upon expansion to

$$\begin{aligned} \varepsilon &= \frac{w_{net}}{(a_{out} - a_{in})_{heat-addition}} \\ &= \frac{w_{net}}{q_{in} - T_o(s_{out} - s_{in})_{heat-addition}} \end{aligned} \quad (9)$$

indicating that for the same heat input and work output, ε would be higher for the terrestrial cycle than the space one because of the much higher assumed T_o , and thus the much lower exergy of the heat input. Looking at it in another way, choice of the very low T_o as it is in space brings the exergy efficiency very close to the energy efficiency. Because the dead state of terrestrial cycles is at $T_o=288.2$ K, the cycle has utilized all of the heat available relative to its surroundings. In space, the heat sink is much lower, reducing the exergy efficiency to approximately the value of the energy efficiency. This shows that it is possible to decrease the low temperature of the space cycle, which will lead to improvements in the efficiency.

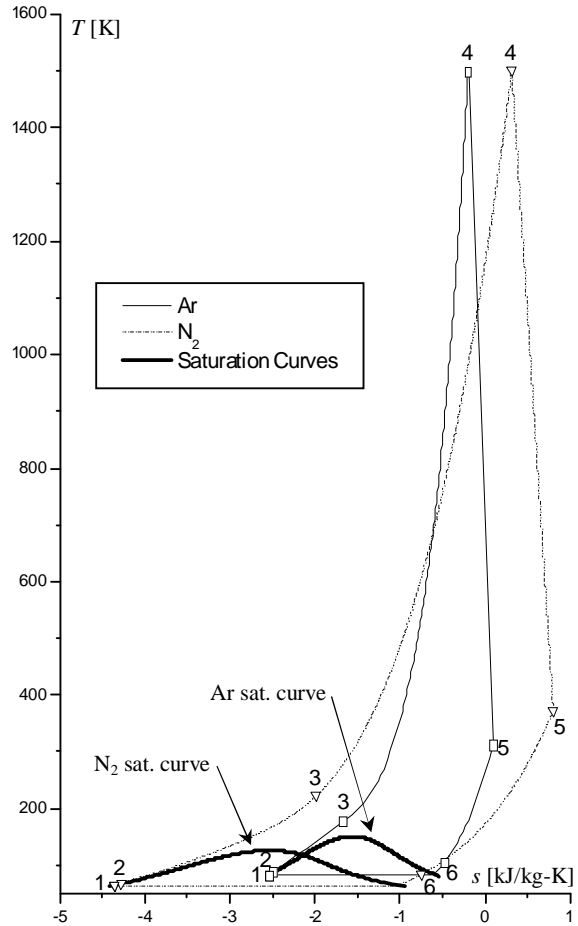


Fig. 9: Rankine cycle T - s diagram
 Ar: $p_L=0.75$ bar, $\pi=200$
 N_2 : $p_L=0.15$ bar, $\pi=1000$

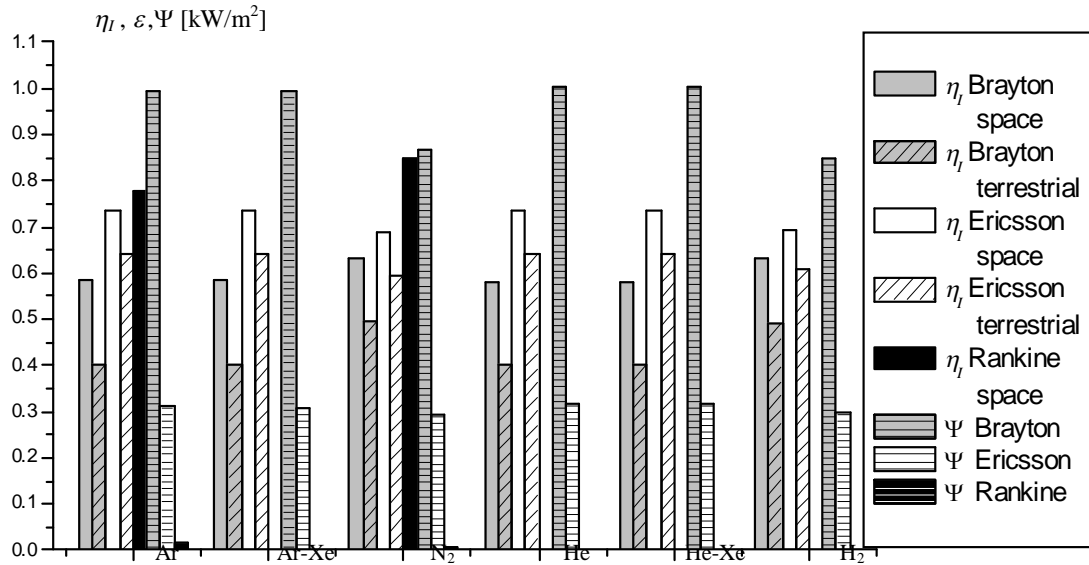


Fig. 10 Computed η_t , ε , and Ψ of the space and terrestrial cycles for the different working fluids. Note: Ψ for the Rankine cycle was computed only for Ar and N₂ and is imperceptibly small here, the values are in Table 2.

For the Brayton cycle, Ψ for N₂ and H₂ is about 14% lower than that of the other working fluids. It can be explained by using Eq. (8): η_t for these fluids is 8% higher because the bottom temperatures are lower, but that also increases the thermal resistance of the radiator by about 30% as well as the temperature difference ΔT_{lm} , resulting in the observed overall reduction of Ψ . For Ericsson cycles, the Ψ relationship to η_t is opposite. These increases in U and ΔT_{lm} are stronger than the effect of the efficiency in Eq. (8) which causes Ar to have higher Ψ than N₂ in the Rankine cycle.

The Rankine cycle has the highest exergy efficiencies because its T_L is closest to the dead state (Table 2), and Brayton cycles have the lowest because they operate furthest from the dead state. Brayton cycle efficiencies can be improved by lowering the T_L of the cycles. Ericsson cycles have higher ε than Brayton due to higher η_t , but lowering the cycle T_L is difficult because it approaches saturation temperature for Ar, Ar-Xe, and N₂ due to the temperature difference between interstages in the compressor during intercooling stages (Fig. 8).

CONCLUSIONS

1. Under the examined conditions, the thermal efficiency of Brayton cycles reaches 58-63%, Ericsson 69-74%, and Rankine 78-85% (see Fig 10).

2. These efficiencies are significantly higher than those for the computed or real terrestrial cycles: by up to 45% for the Brayton, 17% for the Ericsson, and remarkably 44% for the Rankine cycle even when compared with the best terrestrial combined cycles.

3. From the considered working fluids, the diatomic gases (N₂ and H₂) produce somewhat better efficiencies than the monatomic ones in the Brayton and Rankine cycles, and somewhat lower efficiencies in the Ericsson cycle.

4. Although Rankine cycles have higher thermal and exergy efficiencies, they require much larger radiator areas. As a result, the Rankine cycles on average have lower Ψ , approximately 4% of that obtained for Ericsson cycles and only 1% of that for Brayton cycles.

REFERENCES

- [1] Glaser PE, Davidson FP, Csigi KI. *Solar Power Satellites – the emerging energy option*. New York: Ellis Horwood, 1994.
- [2] Mankins JC. *Space solar power: A major new energy option?* J. Aerospace Engng 2001; 14(2): 38-45.
- [3] Lior N. *Power from space*. Energy Conversion and Management 2001; 42(15-17): 1769-1805.
- [4] Hoffert MI, Caldeira K, Nozette S. *Evolutionary Paths to Orbital Power & Light*. 50th Int. Astronautical Cong., 1999.

- [5] Strickland JK. Advantages of solar power satellites for base load electrical supply
- [6] Canough G. *Space solar power vs. terrestrial solar power*. Space Energy& Transportation 1997; 2(2): 155-127.
- [7] Nagatomo M. *An approach to develop space solar power as a new energy system for developing countries*. Solar Energy 1996; 56(1): 111-118.
- [8] Glaser PE. *Guest editorial: Solar energy for planet Earth*. Solar Energy 1996;56(1): 1-2.
- [9] Harper, W.B., Boyle, .B., Kudija, C.T. *Solar dynamic CBC power power for space station Freedom*, ASME paper 90-GT-78, NY,1990.
- [10] Wu, Yu-Ting, Ren, Jian-Xun, Guo, Zeng-Yuan, Liang, Xin-Gang, Optimal analysis of a space solar dynamic power system. Solar Energy, 2003; 74(3):205-215.
- [11] Assis AKT, Neves MCD. *History of 2.7 K Temperature Prior to Penzias and Wilson*. APEIRON 1995; 2(3): 79-84.
- [12] NASA Goddard Space Flight Center <http://library.gsfc.nasa.gov/GSFCHome.htm>
- [13] Nichols, L.D. *Comparison of Brayton and Rankine cycle magnetogasdynamic space-power generation systems*, NASA TN D-5085, NASA, Washington, D.C. March 1969.
- [14] Thomas S. *Effects of the Earth Orbit environment on thin-wall bubbles*. J. Spacecraft&Rockets 1990; 27(4): 438-445.
- [15] Shaltens RK Boyle RV. Initial results from the solar dynamic (SD) ground test demonstration (GTD) project at NASA Lewis. Proc. 30th IECEC ASME, Orlando, 1995.
- [16] Shepard NF et al. 20-kWe space reactor power system using Brayton cycle conversion. Proc. 11th Symp. on Space Nuclear Power and Propulsion, Albuquerque, NM, USA,1994.
- [17] Agazzani A, Massardo A. *Advanced solar dynamic space power systems, Part I: efficiency and surface optimization*. ASME Journal of Solar Energy Engng, 1995; 117(4): 265-274
- [18] Agazzani A, Massardo A. *Advanced solar dynamic space power systems, Part II: Detailed Design and Specific Parameters Optimization*. ASME J. Solar Energy Engng 1995; 117(4): 274-281.
- [19] Hanlon C. *Feasibility of Demonstration Solar Dynamics on Space Station*. Proc. 29th IECEC Part 2, 1994.
- compared to ground solar power. Solar Energy 1996; 56(1): 23-40.
- [20] Shaltens RK, Mason LS. *Early Results from Solar Dynamic Space Power System Testing*. J. Propulsion&Power 1996; 12(5): 852-858.
- [21] Aspen Plus[®], Aspen Technology, Inc., version 12.1, <http://www.aspentech.com/>
- [22] Rukes B, Taud R. *Status and perspectives of fossil power generation*. Energy 2004; 29(12-15): 1853-1874.
- [23] Valenti M. *Reaching for 60 percent*. Mechanical Engineering 2002; 124(4): 35-39.